



**HAL**  
open science

# Optimization Study of a NODA Derivative Radiofluorination by A118F Complexation Using a Design of Experiments Approach

Carine San, Benoît Hosten, Nicolas Vignal, Meriem Beddek, Maurice Pillet,  
Laure Sarda-Mantel, Marc Port, Fabienne Dioury

► **To cite this version:**

Carine San, Benoît Hosten, Nicolas Vignal, Meriem Beddek, Maurice Pillet, et al.. Optimization Study of a NODA Derivative Radiofluorination by A118F Complexation Using a Design of Experiments Approach. *Chemistry - A European Journal*, 2023, 10.1002/chem.202302745 . hal-04230106

**HAL Id: hal-04230106**

**<https://cnam.hal.science/hal-04230106v1>**

Submitted on 5 Oct 2023

**HAL** is a multi-disciplinary open access archive for the deposit and dissemination of scientific research documents, whether they are published or not. The documents may come from teaching and research institutions in France or abroad, or from public or private research centers.

L'archive ouverte pluridisciplinaire **HAL**, est destinée au dépôt et à la diffusion de documents scientifiques de niveau recherche, publiés ou non, émanant des établissements d'enseignement et de recherche français ou étrangers, des laboratoires publics ou privés.

# Excellence in Chemistry Research

## Announcing our new flagship journal

- Gold Open Access
- Publishing charges waived
- Preprints welcome
- Edited by active scientists



## Meet the Editors of *ChemistryEurope*



**Luisa De Cola**

Università degli Studi  
di Milano Statale, Italy



**Ive Hermans**

University of  
Wisconsin-Madison, USA



**Ken Tanaka**

Tokyo Institute of  
Technology, Japan

# Chemistry A European Journal

 **Chemistry  
Europe**  
European Chemical  
Societies Publishing

## Accepted Article

**Title:** Optimization Study of a NODA Derivative Radiofluorination by Al<sup>18</sup>F Complexation Using a Design of Experiments Approach

**Authors:** Carine San, Benoît Hosten, Nicolas Vignal, Meriem Beddek, Maurice Pillet, Laure Sarda-Mantel, Marc Port, and Fabienne Dioury

This manuscript has been accepted after peer review and appears as an Accepted Article online prior to editing, proofing, and formal publication of the final Version of Record (VoR). The VoR will be published online in Early View as soon as possible and may be different to this Accepted Article as a result of editing. Readers should obtain the VoR from the journal website shown below when it is published to ensure accuracy of information. The authors are responsible for the content of this Accepted Article.

**To be cited as:** *Chem. Eur. J.* **2023**, e202302745

**Link to VoR:** <https://doi.org/10.1002/chem.202302745>

## RESEARCH ARTICLE

# Optimization of a NODA Derivative Radiofluorination by Al<sup>18</sup>F Complexation Using a Design of Experiments Approach

Carine San<sup>\*[a,b]</sup>, Benoît Hosten<sup>[b,c]</sup>, Nicolas Vignal<sup>[b]</sup>, Meriem Beddek<sup>[b]</sup>, Maurice Pillet<sup>[d]</sup>, Laure Sarda-Mantel<sup>[b]</sup>, Marc Port<sup>[a]</sup>, Fabienne Dioury<sup>\*[a]</sup>

[a] Dr C. San, Prof M. Port, Dr F. Dioury

Laboratoire GBCM, EA7528, Conservatoire National des Arts et Métiers, HESAM Université,  
2 rue Conté, 75003 Paris (France)

E-mail: [carine.san@lecnam.net](mailto:carine.san@lecnam.net); [fabienne.dioury@lecnam.net](mailto:fabienne.dioury@lecnam.net)

[b] Dr C. San, Dr B. Hosten, Dr N. Vignal, M. Beddek, Prof L. Sarda-Mantel

Unité Claude Kellershohn, Institut de Recherche Saint-Louis, Hôpital Saint-Louis, Université Paris Cité,  
1 avenue Claude Vellefaux, 75010 Paris (France)

[c] Dr B. Hosten

INSERM UMR-S 1144, Optimisation Thérapeutique en Neuropsychopharmacologie, Université Paris Cité,  
4 avenue de l'Observatoire, 75006 Paris (France)

[d] Prof M. Pillet

Laboratoire SYMME, EA 4144, Université Savoie Mont-Blanc,  
7 chemin de Bellevue, 74940 Annecy (France)

Supporting information for this article is given via a link at the end of the document.

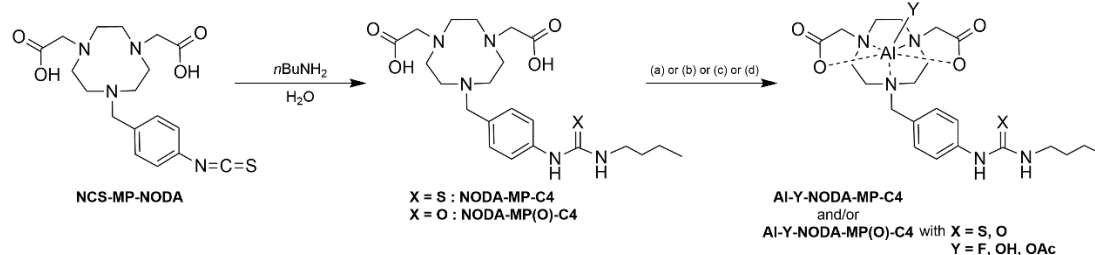
**Abstract:** Fluorine-18 (<sup>18</sup>F) is the most favorable positron emitter for radiolabeling Positron Emission Tomography (PET) probes. However, conventional <sup>18</sup>F labeling through covalent C-F bond formation is challenging, involving multiple steps and stringent conditions unsuitable for sensitive biomolecular probes whose integrity may be altered. Over the past decade, an elegant new approach has been developed involving the coordination of an aluminum fluoride {Al<sup>18</sup>F} species in aqueous media at a late-stage of the synthetic process. The objective of this study was to implement this method and to optimize radiolabeling efficiency using a Design of Experiments (DoE). To assess the impact of various experimental parameters on {Al<sup>18</sup>F} incorporation, a pentadentate chelating agent NODA-MP-C4 was prepared as a model compound. This model carried a thiourea function present in the final conjugates resulting from the grafting of the chelating agent onto the probe. The formation of the radioactive complex Al<sup>18</sup>F-NODA-MP-C4 was studied to achieve the highest radiochemical conversion. A complementary "cold" series study using the natural isotope <sup>19</sup>F was also conducted to guide the radiochemical operating conditions. Ultimately, Al<sup>18</sup>F-NODA-MP-C4 was obtained with a reproducible and satisfactory radiochemical conversion of 79 ± 3.5% (n = 5).

## Introduction

Positron emission tomography (PET) is an imaging technique that provides non-invasive, sensitive and specific imaging of molecular processes *in vivo*. PET imaging is nowadays widely used in clinical routine, particularly in oncology, as this molecular imaging modality gives access to quantitative information on tumor evolution. This technique requires to inject a radiopharmaceutical at concentration subtherapeutic dose (nano or picomolar range) which is labelled with a radionuclide such as

carbon-11 (<sup>11</sup>C), fluorine-18 (<sup>18</sup>F) or gallium-68 (<sup>68</sup>Ga). Among these positron ( $\beta^+$ ) emitters, <sup>18</sup>F remains the most favorable positron emitter due to its advantageous nuclear properties – the longer half-life ( $t_{1/2}$  = 110 min), the "purest" amount of  $\beta^+$  decay (96.7%) and the lower maximum  $\beta^+$  energy, ( $E_{\beta+\max}$  = 634 keV) – making <sup>18</sup>F-PET imaging more sensitive and more resolute compared to <sup>11</sup>C- ( $t_{1/2}$  = 20.4 min, 99.8%  $\beta^+$  emitter,  $E_{\beta+\max}$  = 960 keV) or <sup>68</sup>Ga-PET ( $t_{1/2}$  = 67.7 min, 88.9%  $\beta^+$  emitter,  $E_{\beta+\max}$  = 1900 keV).<sup>[1]</sup> In addition, <sup>18</sup>F can be produced on a large scale by small medical cyclotrons to serve several hospitals and imaging facilities. Meanwhile, in recent years, immunotherapy and targeted therapy have transformed the landscape of cancer treatment, and a new need has emerged for radiolabeling of sensitive probes such as peptides or proteins, to predict and monitor the response of these new treatments. However, the conventional <sup>18</sup>F-fluorinations, based on a direct covalent C-F bond formation are often cumbersome with multistep procedures performed in rather drastic reaction conditions (anhydrous conditions, organic solvent, organic catalyst, high temperature, non-physiological conditions) that are not compatible with probes which are subject to denaturation. Consequently, over the past decade, alternative radiofluorination methods suitable for peptides or proteins have been explored.<sup>[2,3]</sup> Among them, one of the most studied and extensively applied is based on the coordination of an aluminum-<sup>18</sup>F fluoride species {Al<sup>18</sup>F} with a chelating agent.<sup>[4,5]</sup> The main strength of this procedure is that the radiolabeling step proceeds in aqueous media, is very fast, and is the last step in the radiotracer preparation process. The approach relies on a bifunctional chelating agent previously conjugated to the probe which can capture the Al<sup>18</sup>F generated *in situ* by mixing [<sup>18</sup>F]fluoride with aluminum trichloride. Thus, by combining coordination chemistry and one of the strongest metal-<sup>18</sup>F fluoride species, this elegant approach overcomes the

## RESEARCH ARTICLE



**Scheme 1.** Synthesis of the chelating agents discussed herein and of the corresponding aluminum chelates. (a) for X = S, Y = F:  $\text{AlCl}_3$ , NaF, AcONa/H buffer ( $\text{pH}$  4.5, 0.1M), EtOH, aq. NaOH,  $100^\circ\text{C}$ , 15 min. (b) for X = S or O, Y = OH:  $\text{AlCl}_3$ , aq. NaOH to final  $\text{pH}$  4.7-5.0,  $100^\circ\text{C}$ , 1.5 h. (c) for X = S, Y = OH, OAc (mixture):  $\text{AlCl}_3$ , AcONa/H buffer ( $\text{pH}$  4.5, 0.1M), EtOH,  $100^\circ\text{C}$ , 30 min then r.t. overnight. (d) for X = O, Y = F, OAc (mixture):  $\text{AlCl}_3$ , NaF, AcONa/H buffer ( $\text{pH}$  4.45, 0.5M), EtOH,  $100^\circ\text{C}$ , 20 min.

stringent conditions of the covalent C-F bond radiofluorinations applied to small probes such as  $^{18}\text{F}$ FDG. Among the chelating agents previously explored for  $\text{Al}^{18}\text{F}$  complexation, it is now of common knowledge that the pentadentate 1,4,7-triazacyclononane-1,4-diacetic acid (NODA) is the “gold standard” chelator for the complexation of  $\text{Al}^{18}\text{F}$  species.<sup>[6]</sup> Several  $\text{Al}^{18}\text{F}$ -NODA radiofluorinations have been reported in the literature<sup>[7–10]</sup> and all optimizations studies have been performed by using the one variable (factor) at a time (OV(F)AT) approach.<sup>[11,12]</sup> Although easy to implement, this more conventional and scientific intuition-based approach does not detect potential interactions between factors and may lead to a false optimum response. Furthermore, an efficient process optimization technique is essential in the particular case of a radiosynthesis step that is highly dependent on compliance with radiation protection regulations.

In this context, the design of experiments (DoE) optimization approach is particularly relevant, as it enables us to model a response (radiochemical conversion (RCC),<sup>[13]</sup> for example) in a multidimensional experimental space determined by the most important influencing factors and their range of variability, on the basis of a reduced number of tests judiciously selected using DoE software. Reducing the number of tests to be carried out not only saves material resources and experimentation time, but also, and above all, reduces operator exposure to ionizing radiation, especially as such optimization studies are generally performed manually. Finally, another benefit of using a DoE is to provide a predictive mathematical model that takes into account the possible interactions between factors and/or the possible quadratic effects of some factors, in order to obtain the optimal experimental protocol. In this study, we present an optimization based on this statistical method using the NODA-derived chelating agent NODA-MP-C4 (Scheme 1) as model for the capture of  $\text{Al}^{18}\text{F}$ .

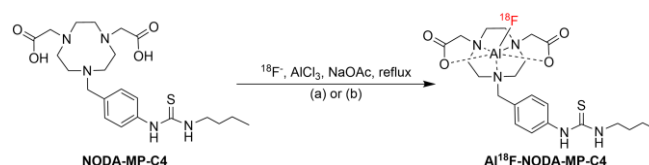
## Results and Discussion

### Preliminary Radiofluorination and Analytical Optimization

$\{\text{Al}^{18}\text{F}\}$  coordination was studied on the model compound NODA-MP-C4, a derivative of the extensively used and commercially available bifunctional chelator NCS-MP-NODA (Scheme 1).<sup>[8,14–17]</sup> NODA-MP-C4 was easily obtained by reaction with an excess of *n*-butylamine in warmed water (92%). It is

interesting to note that the prior alkalization of the reaction medium carried out to solubilize the diacetic precursor in water was detrimental and led to a mixture of the desired thiourea together with its oxygen analogue (urea) NODA-MP(O)-C4 (Scheme 1). Interestingly, this side product was also found in the radiosynthesis media and consequently was used to prepare analytic references.

Based on reported protocols,<sup>[5,8,17]</sup> a preliminary radiolabeling with NODA-MP-C4 was performed (Scheme 2). A fluoride-18 solution obtained by quaternary methyl ammonium (QMA) cartridge purification was mixed with a  $\text{AlCl}_3$  solution (30  $\mu\text{L}$ , 2mM) in AcONa/H buffer (0.1M,  $\text{pH}$  4.0) and a NODA-MP-C4 solution (30  $\mu\text{L}$ , 2mM) in AcONa/H buffer (0.1M,  $\text{pH}$  4.0). This mixture was heated at reflux ( $100^\circ\text{C}$ ) for 25 min. Initially, a short reversed phase HPLC column was used (Kinetex C18, 50 mm x 2.1 mm – 2.6  $\mu\text{m}$ ) to benefit from shorter duration of analysis (Figure 1a), smaller injection volume and a reduction of operator radiation exposition. However, first tests were not conclusive as resolution of the radiochromatogram used to follow the radiofluorination was rather poor (Figure 1b). This chromatographic resolution issue has been solved by increasing the length of the column (Kinetex Evo C18, 100 mm x 4.6 mm – 5  $\mu\text{m}$ ) to improve the number of theoretical plates, while ensuring a suitable analysis time for monitoring successive tests as part of an optimization strategy (Figure 1c). This improvement in the chromatographic resolution made it possible to detect several peaks on both the UV and the radiochromatograms (Figures 1c-1d). The presence of several peaks suggests side reactions. Indeed, the thiourea motif as a bioconjugation link may be subject to degradation processes (radiolysis, hydrolysis, etc) which are sometimes reported, rarely quantified, but strongly dependent of the presence of a potential neighboring participation group.<sup>[5,18,19]</sup> In order to identify the nature of the side products found in the media, a reversed-phase LC-MS study of some crude radiofluorination media was performed after radioactive decay.



**Scheme 2.** Radiofluorination of NODA-MP-C4 by  $\text{Al}^{18}\text{F}$ . a) Preliminary test: 0.1 M AcOH/Na buffer  $\text{pH}$  4.0,  $[\text{NODA-MP-C4}] = 550 \mu\text{M}$ ,  $[\text{NODA-MP-C4}/\text{AlCl}_3 \text{ ratio}] = 1/1$ , 25 min; b) DoE optimization tests (see Table 1): 0.1 M AcOH/Na buffer  $4.0 < \text{pH} < 5.0$ ,  $[\text{NODA-MP-C4}] = 55$  to  $550 \mu\text{M}$ ,  $[\text{NODA-MP-C4}/\text{AlCl}_3 \text{ ratio}] = 1/1$  to  $3/1$ , 15 min.

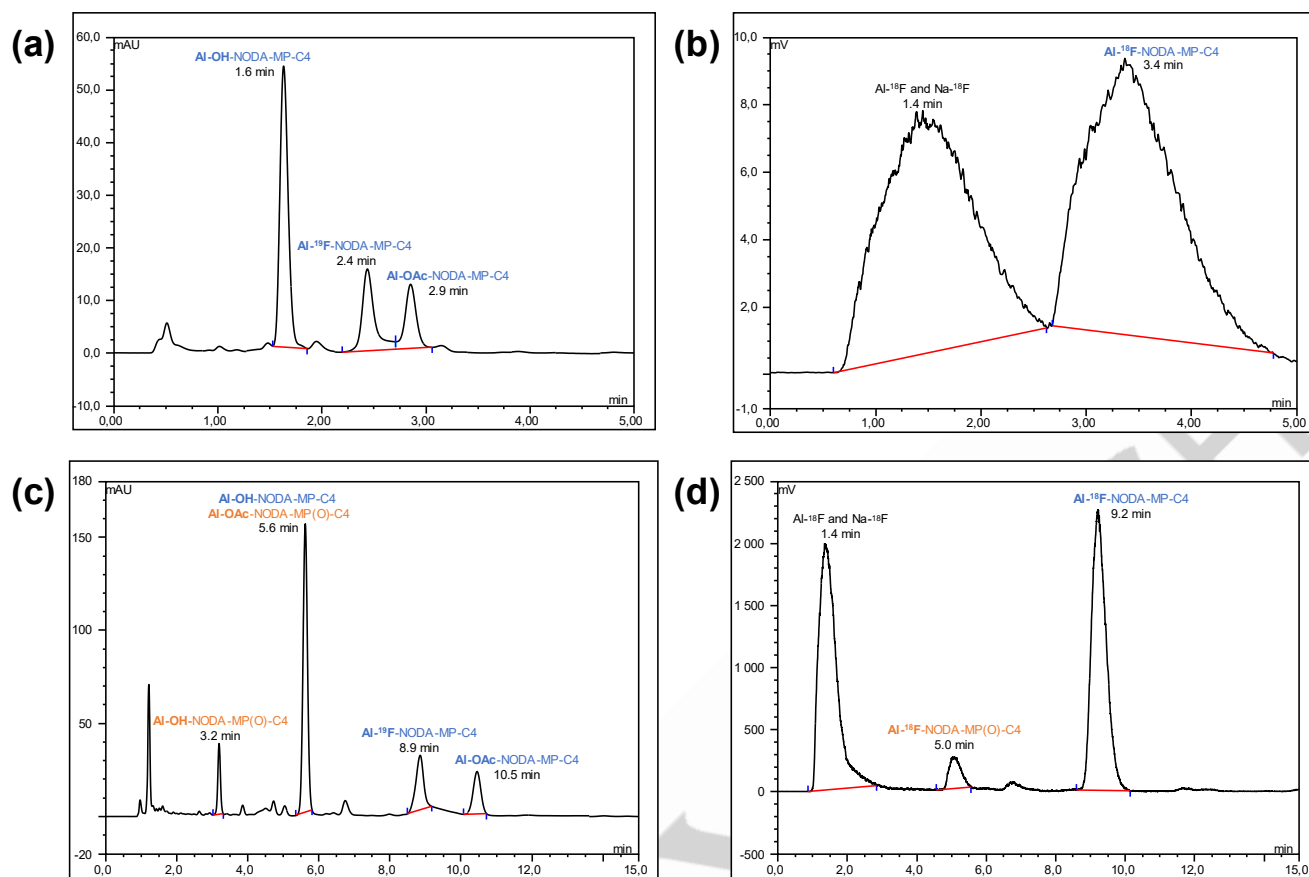


**Figure 1.** Optimization of the RP-HPLC method: chromatograms obtained with: (up) a Phenomenex Kinetex C18, 50 mm x 2.1 mm – 2.6  $\mu$ m column; mobile phase: acetate buffer pH 4.5 / MeCN 85/15, isocratic mode, flow rate: 0.4 mL/min, injection volume: 2.5  $\mu$ L and (a) diode-array detector (PDA) (254 nm) or (b) radio detector; (down) with a Phenomenex Kinetex Evo C18, 100 mm x 4.6 mm – 5  $\mu$ m column; mobile phase: acetate buffer pH 4.5 / MeCN 85/15, isocratic mode, flow rate: 1 mL/min, injection volume: 25  $\mu$ L, and (c) PDA (254 nm) or (d) radio detector; the difference in retention time ( $R_t$ ) results from the dead volume between the two detectors (0.3 min with this method).

Several degradations of the chelator can be hypothesized: 1/ radiolytic and/or acid-assisted cleavages of the methylphenyl or thiourea bond leading respectively to NODA, NODA-MP-NH<sub>2</sub>,<sup>[17]</sup> and NODA-MP-NHCSNH<sub>2</sub> derivatives (Figure 2) and 2/ transformation of the thiourea function into a urea function to give NODA-MP(O)-C4 derivatives (Scheme 1). These compounds and their Al(III) complexes were prepared to provide analytical references for this investigation (see Supporting Information). Based on LC-MS of the synthetic references, radio- and/or hydrolytic side products were found to be eluted in the dead volume; only NODA-MP(O)-C4 and its corresponding Al(III) complexes were able to be identified in HPLC chromatograms. Despite the side products observed in this preliminary experiment, the 45% RCC obtained can be compared with that obtained by Shetty and al. with the NCS-MP-NODA derivative resulting from its conjugation to the RGD tripeptide (58%).<sup>[17]</sup> To improve this preliminary conversion, optimization using a DoE methodology was considered.

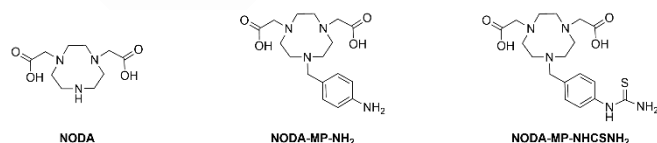


**Figure 2:** Chemical structure of the ligands potentially resulting from the degradation of NODA-MP-C4

### Radiolabeling Optimization by DoE Approach

Since the literature reviews have highlighted most of the main significant factors impacting on the RCC by Al<sup>18</sup>F such as pH, chelator concentration, reaction temperature,<sup>[5,20]</sup> it did not seem relevant to carry out a factorial screening design as it provides limited information on the interactions between factors and a less accurate predictive model. Consequently, a response surface design was selected in order to achieve a more detailed view of the contribution of each factor to the radiochemical conversion. This design provides better resolution and quality on information but requires more experimental conditions per factor. We have therefore decided to limit ourselves to three factors, as a higher number of factors requires a large number of runs associated with a lot of experimental time, which calls into question the interest in using a DoE methodology: i) the pH of the medium (ranging from pH 4.0 to pH 5.0); ii) the concentration of the chelating agent ([NODA-MP-C4] ranging from 55 to 550  $\mu$ M); iii) the ratio of the chelating agent to the metal precursor AlCl<sub>3</sub> (NODA-MP-C4 / AlCl<sub>3</sub> ranging from 1/1 to excess of chelating agent up to 3/1). Other significant factors such as time, temperature, reaction volume and addition of organic cosolvent (ethanol) were set. Based on optimization studies reported in the literature,<sup>[8–10,17]</sup> temperature was set to reflux of the buffered aqueous medium (100°C), and the reaction volume was set to the minimum possible, which was in our case 110  $\mu$ L due to our experimental equipment.

## RESEARCH ARTICLE

**Table 1.** DoE generated by Ellistat® software and radiochemical conversion obtained for each test.

Nb	NODA-MP-C4 / AlCl <sub>3</sub> ratio	[NODA-MP-C4] (μM)	pH	Radiochemical conversion (%)	
				Series A	Series B
1	1.4 / 1	156	4.2	27	54
2	1.4 / 1	156	4.8	45	52
3	1.4 / 1	450	4.2	76	75
4	1.4 / 1	450	4.8	75	72
5	2.6 / 1	156	4.2	22	26
6	2.6 / 1	156	4.8	13	20
7	2.6 / 1	450	4.2	30	68
8	2.6 / 1	450	4.8	42	69
9	2 / 1	303	4.5	71	67
10	2 / 1	303	4.5	56	63
11	2 / 1	303	4.5	56	63
12	2 / 1	303	4.5	70	64
13	2 / 1	303	4.5	72	59
14	2 / 1	303	4.5	71	71
15	1 / 1	303	4.5	70	75
16	3 / 1	303	4.5	50	61
17	2 / 1	55	4.5	2	14
18	2 / 1	550	4.5	64	74
19	2 / 1	303	4	16	20
20	2 / 1	303	5	18	27

Preliminary studies were carried out to determine the time and the proportion of co-solvent. Time was set at 15 minutes as no conversion improvement was observed by extending the reaction time (Figure S1). Regarding the influence of ethanol as a co-solvent, no effect was observed on our system by varying its proportion from 0 to 60% (Figure S2). Furthermore, since the addition of ethanol can have an impact on the pH of the medium, we decided to perform this optimization in a 0.1M AcONa/H buffered aqueous medium without any addition of organic co-solvent (Scheme 2). Once the factors and the study domain had been determined, the DoE software (Ellistat®) generated a series of 20 tests (Table 1, Series A) to be carried out. This series was duplicated to increase the robustness of the model (Table 1, Series B). Each couple of tests (Nb *iA* and *iB*, with *i* = 1 to 20) were performed on different days to take into account the

variability in the quality of the fluorine-18 delivered. The experimental results (RCC obtained for each DoE test) are used to generate a mathematical model of the response surface design. This model is an equation that predicts the output (i.e. RCC) as a function of the experimental inputs, in this case the three reaction factors previously discussed and allowed to vary (Equation 1). In the model, the coefficient of each factor, also known as regression factor, reflects the extent of its impact on RCC (Figure 3a). To confirm their significant impact, a t-test was performed on the regression factors scaled and centered (Table S1). For the system studied, on the basis of the *p*-value, the three factors left variable have a significant impact on the RCC (*p* < 0.05). Moreover, this model revealed quadratic effects for the pH and the concentration of chelating agent [NODA-MP-C4], meaning that these factors have nonlinear effect on RCC (Figure 3c). These nonlinear effects could not have been detected without a response surface design, which validates our strategy for the choice of this experimental design. In addition, no interaction between the three factors was found significant. Figure 3b indicates that the model is highly predictive since the adjusted R<sup>2</sup> and the predicted R<sup>2</sup> are 81.8% and 73.1% respectively. To validate the robustness of the model, additional tests, different from the 20 tests planned by the DoE, were carried out. This was done with two points of the response surface design: one anywhere in the study domain not included in the DoE, the second one corresponding to the predicted optimum conditions. The first validation test was carried out at pH = 4.3, with a chelating agent concentration [NODA-MP-C4] set to 223 μM, in the presence of an excess of chelating agent defined by the ratio NODA-MP-C4 / AlCl<sub>3</sub> = 1.8 / 1. This test was triplicated and performed on two non-consecutive days; RCCs of 67, 58 and 66% were obtained (64 ± 4.5% (n=3)) for a predicted value of 51%. The second validation test under optimal predicted conditions (pH = 4.5, [NODA-MP-C4] = 465 μM, ratio NODA-MP-C4 / AlCl<sub>3</sub> = 1 / 1) was repeated five times over a period of one year; an experimental RCC of 79 ± 3.5% (n = 5) was obtained for a predicted value of 90% (Figure 4). For both validation tests, the standard deviation was inferior to 2σ, meaning the model calculated is satisfactory. Moreover, repeated tests carried out under optimum conditions demonstrated the reproducibility of the radiolabeling protocol. To our knowledge, this protocol achieved the highest RCC ever obtained with a similar system (i.e. chelating agent of NODA-type). This was made possible by using a response surface design that provides a more complete behavior of each factor allowed to vary. Indeed, more condition levels are studied for each factor unlike screening factorial design. Finally, we were able to show the nonlinear effect of pH and the concentration of the chelating agent [NODA-MP-C4] and consequently, to determine the “true” optimum. Interestingly, under the predicted optimum conditions, the recommended optimum NODA-MP-C4 / AlCl<sub>3</sub> ratio is 1 / 1, which is very advantageous compared to other optimization studies reported in the literature where up to a 5-fold excess of the chelating agent compared to Al<sup>3+</sup> was recommended.<sup>[20]</sup>

*Radiochemical conversion*

$$= - 3235 - 14,99 \times \text{NODA} - \text{MP} - \text{C4} / \text{AlCl}_3 + 0,3316 \times [\text{NODA} - \text{MP} - \text{C4}] + 1477 \times \text{pH} - 0,0003614 \times [\text{NODA} - \text{MP} - \text{C4}]^2 - 160,4 \times \text{pH}^2$$

**Equation 1.** Mathematical model generated by Ellistat® software of the response surface design

## RESEARCH ARTICLE

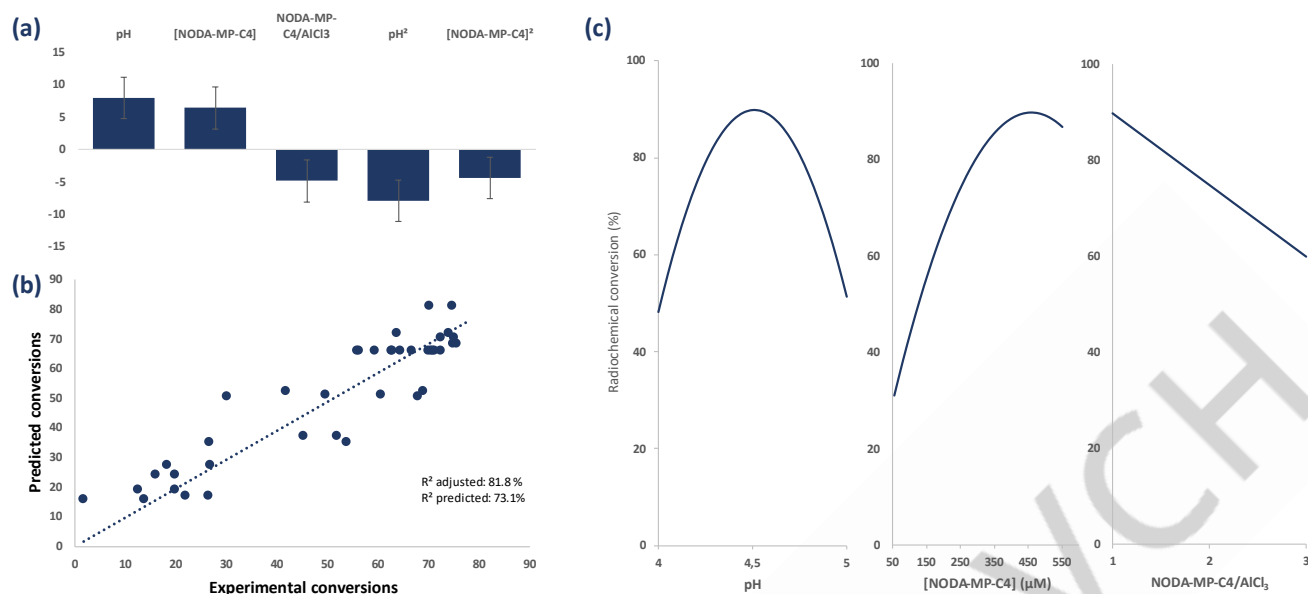


**Figure 3.** DoE results: (a) scaled and centered regression factors representing the contribution of each factor on the RCC, (b) fitness of the model generated by the data and software and (c) impact of each factor on the RCC.

Careful selection of the studied factors is essential for effective process optimization using a DoE methodology. For the system studied here, a response surface design could be carried out because radiolabeling by coordination of  $\text{Al}^{18}\text{F}$  is widely described and the main factors impacting RCC have therefore already been identified. The DoE methodology is particularly relevant for systems, such as the one studied here, for which a high variability of the results is obtained, as the DoE has led to a predictive model whose accuracy and robustness remain satisfactory. In this work, the predictive model and optimal reaction conditions are valid only for NODA-MP-C4. However, the factors selected for this DoE approach are also relevant for optimizing radiolabeling of other NODA-derived chelators, especially for NODA-biomolecule conjugated compounds with potential clinical applications. Therefore, a response surface model can be rapidly implemented for efficient and reliable optimization. We believe that employing the DoE approach is a more appropriate strategy than OVAT in this context. Not only may it require fewer tests, but it also provides a better understanding of the influence of these factors on radiochemical conversion as well as delivering a predictive model that is unavailable by the conventional OVAT approach.

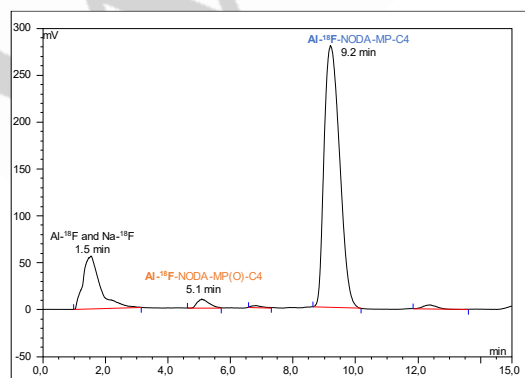


**Figure 4.** Representative radiochromatogram of  $\text{Al}^{18}\text{F}$ -NODA-MP-C4 ( $R_t = 9.2$  min) radiolabeling with optimal conditions ( $\text{pH} 4.5$ ,  $[\text{NODA-MP-C4}] = 465 \mu\text{M}$  and  $\text{NODA-MP-C4} / \text{AlCl}_3$  ratio = 1 / 1).

## Conclusion

This study highlights the formation of side products during radiofluorination by complexation of  $\text{Al}^{18}\text{F}$  with the NODA-MP-C4 chelator. It reports for the first time the optimization of radiolabeling with  $\text{Al}^{18}\text{F}$  performed using a DoE methodology. This type of statistical approach allows different levels of optimization depending on the level of knowledge of the process studied. For radiolabeling with the NODA-MP-C4 chelating agent, optimization by DoE proved effective for the following reasons: *i/* a reduced number of tests (40 assays performed in 5 days of experimentation) resulting in significant improvement in RCC (45% vs 79%), *ii/* the possibility of identifying potential interactions between factors, and *iii/* the generation of a predictive model to obtain high and reproducible conversion ( $79 \pm 3.5\%$  ( $n = 5$ )). Recent studies have shown that acyclic chelators coordinate  $\text{Al}^{18}\text{F}$  at lower temperature (room temperature) than NODA-based cyclic chelator. Even if the *in vivo* stability of these chelators is still debated in the literature to estimate their actual applicability as a new tool for targeted tracer labeling for PET imaging<sup>[20,21]</sup>, these recent results demonstrated that there is still room for the development of alternative radiolabeling systems. DoE approach to optimize radiosynthesis processes of these new chelators could probably be of great interest. Finally, as radiolabeling optimization is often performed manually, the DoE approach seems relevant as it reduces the number of tests and, consequently, operator's exposure to ionizing radiation.



## RESEARCH ARTICLE

## Experimental Section

## General

NCS-MP-NODA (CAS RN 1374994-81-6) was purchased from Chematech as a monohydrate form (ref C110, C<sub>18</sub>H<sub>24</sub>N<sub>4</sub>O<sub>4</sub>S·H<sub>2</sub>O). Aluminum chloride hexahydrate (AlCl<sub>3</sub>·6H<sub>2</sub>O), sodium acetate and acetic acid were purchased from Sigma Aldrich. Free metals trace products were purchased, and synthesis were prepared in metal free containers to avoid metal contamination. Ultrapure H<sub>2</sub>O (resistivity 18.2 MΩ·cm at 25 °C) was obtained from a water purification system (MilliQ or Micropure). Solid-phase extraction cartridges (Sep-Pak Light Accell Plus QMA Plus Light) were purchased from Waters™. Fluorine-18 was produced from cyclotron (Cyclone IBA 18/9 cyclotron).

*Thin-layer chromatography (TLC)* were performed on pre-coated aluminum sheets RP-18W / UV<sub>254</sub> (Macherey-Nagel, ref. 818146), and visualized under an UV lamp at 254 nm and/or developed with phosphomolybdic acid stain in ethanol.

*Purifications by flash-chromatography* were conducted on POLYGOPREP® 60-50 C<sub>18</sub> adsorbent purchased from Macherey-Nagel (ref 711500).

*Purifications on preparative RP-TLC glass plates* were conducted on 20x20 cm RP-18 W UV<sub>254</sub> glass plates coated with C18-modified silica layer purchased from Macherey-Nagel, (ref 811074). Desorption of the eluted compounds was obtained by washing the recovered silica band with a solution of H<sub>2</sub>O/MeCN 1/1 v/v, concentration to dryness; the matter obtained was then taken up in pure water and the solution filtered through a PolyEtherSulfone (PES) membrane 0.22 μm (33 mm syringe filter unit, Millex®-GP, Merck, ref SLGP033RS).

*Proton (<sup>1</sup>H), carbon (<sup>13</sup>C) and fluorine (<sup>19</sup>F) NMR spectra* were recorded at 400 MHz (<sup>1</sup>H) on a Bruker spectrometer Avance 400. Carbon NMR (<sup>13</sup>C{<sup>1</sup>H}) spectra were recorded using a broadband decoupled mode with the multiplicities obtained from a DEPT sequence. Chemical shifts (δ) are reported in parts per million (ppm) using the deuterated solvent signals as an internal reference: for D<sub>2</sub>O: <sup>1</sup>H: 4.80 ppm; for DMSO-*d*<sub>6</sub>: <sup>1</sup>H: 2.50 ppm, <sup>13</sup>C: 39.5 ppm. For <sup>19</sup>F{<sup>1</sup>H} NMR, NaF was used as internal reference: D<sub>2</sub>O: -121.1 ppm.<sup>[22]</sup> All spectra were recorded at 298 K. The following abbreviations are used for the proton spectra: s: singlet, d: doublet, t: triplet, q: quartet, m: multiplet, br: broad. For some aromatic protons, second order systems can be observed. The ratio Δδ/J has been used to distinguish between systems AB or AX: if the ratio is less than 10, the spin system is designed « system AB », otherwise the spin system is designed « system AX ». Coupling constants (J) are reported in Hertz (Hz).

*Mass spectroscopy* analyses were performed using ElectroSpray Ionization in positive mode (ESI+).

*Low-resolution mass spectroscopy analyses (LRMS)* were done on an analytic system composed of a LC2030 injection system (Shimadzu) coupled to a Micromass ZQ2000 detector (Waters®). Injections were operated by flow injection mode (FIA) with mobile phase being MeOH, MeCN, water or a mixture on these eluents at a flow rate of 0.5 mL/min. Data were collected in the full scan mode at m/z 200–1500. Detection was done at a cone voltage (CV) giving the least amount of fragmentations (5 to 40 V); mobile phase and CV value are given for each compound.

*High-resolution mass spectroscopy analyses (HRMS)* were performed by direct sample introduction on a LTQ Orbitrap® XL High Definition mass spectrometer (Thermo Scientific®). Data were collected in the full scan mode at m/z 150–1000. The source parameters were as follows: ion spray voltage 4000 V, capillary voltage -35 V, capillary temperature 275 °C, sheath gas flow 10 (a.u.). Data were acquired in high-resolution mode (100,000 FWHM a m/z 500). Data acquisition was managed using Xcalibur™ software (version 2.1.0; Thermo Scientific®).

*Liquid chromatography-high-resolution mass spectrometry (LC-HRMS)* analyses were performed on a Synapt®G2 High Definition MS™ (Q-TOF) mass spectrometer (Waters®) combined with a HPLC system (Waters®). Chromatographic separation was performed on a Kinetex 5 μm EVO C18 100 x 4.6 mm LC column (Phenomenex®, ref 00D-4633-E0) set at 20 °C. Compounds were eluted using isocratic mixture (A/B, 85/15, v/v) with water 10 mM ammonium acetate at pH 4.5 as solvent A, and acetonitrile as solvent B. The flow rate was kept at 1 mL/min for 15 min.

Data were collected in the full scan mode at m/z 50–1200 in positive ion mode (ESI+). The source parameters were as follows: capillary voltage 3500 V, cone voltage 30 V, source temperature 130 °C, desolvation temperature 350 °C, cone gas flow 50 L/h, and desolvation gas flow 900 L/h. Leucine enkephalin (2 ng/mL) was used as the external reference compound (Lock-Spray™) for mass correction. Data were acquired in the so-called resolution mode (20,000 FWHM a m/z 500) with a scan time of 0.2 s. Data acquisition was managed using Waters MassLynx™ software (version 4.1; Waters MS Technologies).

*HPLC and radio-HPLC* were carried out on a Waters® system composed of a 600E pump and a PhotoDiode Array (PDA) detector with Max Plot mode on 220-350 nm range or on a ThermoFisher® Dionex Ultimate 3000 HPLC system equipped with LPG-3400SD pump, WPS-3000SL/TSL autosampler, TCC-3000SD column oven, DAD-3000 detector and coupled with a Eckert Ziegler® Mini-Scan TLC scanner and Flow-Count detector. Separations were obtained using a Kinetex 5 μm EVO C18 100 mm x 4.6 mm LC column purchased from Phenomenex® (ref 00D-4633-E0).

*Method:* Phase A: AcONa/H buffer, pH 4.5 (5 mM). Phase B: MeCN. Mobile Phase: isocratic; Phase A/Phase B: 85/15; flow: 1 mL/min. Sample: solution in water, ca 0.2-0.25 mg/mL; injection volume: 10-25 μL. In such conditions, the dead volume of the system was evaluated by injection of AcONa/H buffer: R<sub>t</sub> 0.95 min.

## Synthesis of Analytical References

**NODA-MP-C4 (di-Na form).** NCS-MP-NODA (199.6 g, 0.486 mmol) was suspended in ultrapure H<sub>2</sub>O (8 mL). *N*-butylamine was then added (120 μL, 1.214 mmol, 2.5 equiv); the resulting mixture reached pH 10.5 and became a clear solution that was gently heated (oil bath temperature 70 °C) for 50 min and then at room temperature for 2 hours. The mixture was concentrated to dryness by freeze-drying. The lyophilizate was taken up in ultrapure H<sub>2</sub>O (2 mL), alkalized by addition of a ca 1 M aqueous solution of NaOH (1 mL, 1 mmol, ca 2 equiv; final pH ≥ 10) and freeze-dried again. The crude material was purified by flash chromatography on RP C18 silica gel (H<sub>2</sub>O/MeCN 8/2 v/v); appropriate product fractions were collected and lyophilized to give the title compound as a white solid (228 mg, 92%). TLC (H<sub>2</sub>O/MeCN 75/25 v/v): R<sub>f</sub> 0.40. <sup>1</sup>H NMR (D<sub>2</sub>O, pH 12, c ≈ 26 mM, Figure S3): δ(ppm) 7.51 (2H, part A of AX system, <sup>3</sup>J = 8.1 Hz, CH<sub>ar</sub>), 7.25 (2H, part X of AX syst, <sup>3</sup>J = 8.1 Hz, CH<sub>ar</sub>), 3.96 (2H, s, CH<sub>2</sub>-Ar), 3.47-3.42 (2H, br m, CH<sub>2</sub>(NHCS)), 3.37 (4H, s, CH<sub>2</sub>-CO<sub>2</sub>), 2.98 (6H, s, N-CH<sub>2</sub>), 2.94-2.78 (6H, br m, N-CH<sub>2</sub>), 1.64-1.49 (2H, m, CH<sub>2</sub>(CH<sub>2</sub>NH)), 1.41-1.26 (2H, m, CH<sub>2</sub>(CH<sub>3</sub>)), 0.90 (3H, t, <sup>3</sup>J = 7.4 Hz, CH<sub>3</sub>). <sup>1</sup>H NMR (DMSO-*d*<sub>6</sub>, c ≈ 54 mM, Figure S4): δ(ppm) 11.07 (<1H, br s, NH), 9.86 (<1H, br s, NH), 7.55 (2H, br s, CH<sub>ar</sub>), 7.24 (2H, br s, CH<sub>ar</sub>), 3.65 (2H, br s, CH<sub>2</sub>-Ar), 3.40 (2H, br s, CH<sub>2</sub>(NHCS)), 2.99 (4H, s, CH<sub>2</sub>-CO<sub>2</sub>), 2.80-1.94 (12H, br m, N-CH<sub>2</sub>), 1.60-1.43 (2H, m, CH<sub>2</sub>(CH<sub>2</sub>NH)), 1.39-1.21 (2H, m, CH<sub>2</sub>(CH<sub>3</sub>)), 0.88 (3H, t, <sup>3</sup>J = 7.3 Hz, CH<sub>3</sub>). <sup>13</sup>C{<sup>1</sup>H} NMR (D<sub>2</sub>O, pH 12, c ≈ 79 mM, Figure S3): δ(ppm) 177.7 (CO, CS), 130.8 (CH<sub>ar</sub>), 125.8 (CH<sub>ar</sub>), 59.2 (CH<sub>2</sub>-Ar), 58.5 (CH<sub>2</sub>-CO<sub>2</sub>), 50.5 (N-CH<sub>2</sub>), 50.1 (N-CH<sub>2</sub>), 49.5 (N-CH<sub>2</sub>), 44.1 (CH<sub>2</sub>(NHCS)), 30.4 (CH<sub>2</sub>(CH<sub>2</sub>NH)), 19.5 (CH<sub>2</sub>(CH<sub>3</sub>)), 13.1 (CH<sub>3</sub>). <sup>13</sup>C{<sup>1</sup>H} NMR (DMSO-*d*<sub>6</sub>, c ≈ 75 mM, Figure S4): δ(ppm) 180.4, 176.1 (CO, CS), 139.8 (Cquat<sub>ar</sub>), 131.6 (Cquat<sub>ar</sub>), 130.0 (CH<sub>ar</sub>), 121.8 (CH<sub>ar</sub>), 63.8 (CH<sub>2</sub>-CO<sub>2</sub>), 60.8 (CH<sub>2</sub>-Ar), 53.0-49.5 (br, N-CH<sub>2</sub>), 43.2 (CH<sub>2</sub>(NHCS)), 30.6 (CH<sub>2</sub>(CH<sub>2</sub>NH)), 19.8 (CH<sub>2</sub>(CH<sub>3</sub>)), 13.8 (CH<sub>3</sub>). LRMS (MeOH, 40 V): m/z 246 [NODA + H]<sup>+</sup>, 466 [M + H]<sup>+</sup>, 488 [M + Na]<sup>+</sup>, 510 [M - H + 2Na]<sup>+</sup>, 532 [M - 2H + 3Na]<sup>+</sup>. HRMS: calculated for [C<sub>22</sub>H<sub>35</sub>N<sub>5</sub>O<sub>4</sub>S + H]<sup>+</sup>, m/z: 466.248801, found, m/z: 466.24696 with z = 1; error: 4.0 ppm. HPLC (Figure S8): R<sub>t</sub> 11.0-12.0 min.

**NODA-MP(O)-C4 (Na form).** NCS-MP-NODA (114 mg, 0.278 mmol) was suspended in ultrapure H<sub>2</sub>O (5 mL). The mixture was alkalized by addition of a ca 1 M aqueous solution of NaOH (600 μL, 0.600 mmol, ca 2.2 equiv) that led to a clear solution of pH 11.7. *N*-butylamine was then added (100 μL, 1.01 mmol, 3.6 equiv) and the resulting mixture was gently heated (oil bath temperature 50 °C) for 1.5 hours then at room temperature overnight. The mixture was concentrated to dryness under reduced pressure. The crude material was taken up in ultrapure H<sub>2</sub>O (2 mL), acidified down to pH 5.7 by the addition of a ca 1 M aqueous solution of

## RESEARCH ARTICLE

HCl, concentrated to dryness, and purified by flash chromatography on RP C18 silica gel (H<sub>2</sub>O/MeCN 8/2 v/v). Fractions were collected to give, in the order of elution: first, the title compound as a yellow powder (38 mg, 0.081 mmol, 29%), followed closely by the elution of the NODA-MP-C4 compound as a whitish solid (78 mg, 0.160 mmol, 57%). TLC (H<sub>2</sub>O/MeCN 7/3 v/v): R<sub>f</sub> 0.50 (NODA-MP(O)-C4); R<sub>f</sub> 0.45 (NODA-MP-C4). <sup>1</sup>H NMR (D<sub>2</sub>O, pH 7): δ(ppm) 7.42 (2H, part A of AB system, <sup>3</sup>J = 8.4 Hz, CH<sub>ar</sub>), 7.31 (2H, part B of AB syst, <sup>3</sup>J = 8.4 Hz, CH<sub>ar</sub>), 4.00 (2H, s, CH<sub>2</sub>-Ar), 3.46-3.26 (4H, br AB system, CH<sub>2</sub>-CO<sub>2</sub>), 3.15-2.64 (14H, several br m, CH<sub>2</sub>-NHCS, NCH<sub>2</sub>), 1.54-1.41 (2H, br m, CH<sub>2</sub>(CH<sub>2</sub>NH)), 1.41-1.26 (2H, m, CH<sub>2</sub>(CH<sub>3</sub>)), 0.89 (3H, t, <sup>3</sup>J = 7.3 Hz, CH<sub>3</sub>). LRMS (MeOH, 40 V): *m/z* 246 [NODA + H]<sup>+</sup>, 450 [M + H]<sup>+</sup>, 472 [M + Na]<sup>+</sup>, 494 [M - H + 2Na]<sup>+</sup>, 516 [M - 2H + 3Na]<sup>+</sup>. HRMS: calculated for [C<sub>22</sub>H<sub>35</sub>N<sub>5</sub>O<sub>5</sub>+H]<sup>+</sup>, *m/z*: 450.271645, found, *m/z*: 450.26987 with *z* = 1; error: 4.0 ppm. HPLC (Figure S8): R<sub>t</sub> 4.3 min.

**AI-F-NODA-MP-C4.** Three stock solutions were prepared in advance, all of them diluted in 0.1 M AcONa/H buffer solution at pH 4.5: i) a 0.0134 M solution of chelating agent NODA-MP-C4 isolated at pH 4.3; ii) a 0.1 M solution of AlCl<sub>3</sub> (resulting pH 3.1); iii) a 0.05 M solution of NaF (resulting pH 4.5). AlCl<sub>3</sub> (275 μL of the stock solution, 27.5 μmol, ca 2.2 equiv) and NaF (275 μL of the stock solution, 14 μmol, ca 1.1 equiv) were first mixed and stirred at room temperature for 30 minutes (resulting pH 3.6). The chelating agent (935 μL of the stock solution, ca 12.5 μmol) was then added, and the mixture was diluted by addition of ethanol (165 μL corresponding to 10% v/v of the total reaction volume). The pH of the mixture being 4.1, it was adjusted to pH 4.5 by careful addition of a 1 M aqueous solution of NaOH (35 μL, 35 μmol, ca 2.8 equiv). The mixture was warmed at reflux (100°C) for 15 min. After cooling to room temperature, the pH was lowered slightly to 4.1, while both MS and HPLC controls showed complete conversion. The mixture was then lyophilized, and the crude material (pale pink solid) was purified on preparative RP-TLC glass plate (H<sub>2</sub>O/MeCN 7/3 v/v). The title compound was recovered from a silica strip corresponding to R<sub>f</sub> 0.22-0.27 ranges (2.5 mg); HPLC control gave 94% purity with the presence of Al-OAc-NODA-MP-C4 (3%). Isolated yield: 40%. <sup>19</sup>F{<sup>1</sup>H} NMR (D<sub>2</sub>O, pH 4, Figure S5): δ -165.4 (saturated solution; no complete solubilisation). <sup>19</sup>F{<sup>1</sup>H} NMR (DMSO-d<sub>6</sub>, Figure S5): δ -169.9. LRMS (MeOH, 40 V): *m/z* 532 [Al-F-L + Na]<sup>+</sup>, 1041 [2(Al-F-L) + Na]<sup>+</sup>. HRMS: calculated for [C<sub>22</sub>H<sub>33</sub>AlFN<sub>5</sub>O<sub>5</sub> + Na]<sup>+</sup>, *m/z*: 532.19504, found, *m/z*: 532.19251 with *z* = 1; error: 1.98 ppm. HPLC: R<sub>t</sub> 8.7-8.9 min.

**AI-OH-NODA-MP-C4.** The previously isolated chelating agent NODA-MP-C4 (di-Na form) (33 mg, ca 65 μmol) was solubilized in ultrapure H<sub>2</sub>O (2.5 mL). AlCl<sub>3</sub>·6H<sub>2</sub>O (30 mg, 125 μmol, 1.9 equiv) was added in one solid portion resulting in the drop of pH from 10.7 to 3.8 and the apparition of a white suspended solid. The pH was adjusted to pH 5.0 by careful addition of a 1 M aqueous solution of NaOH (290 μL, 290 μmol, ca 4.5 equiv). The resulting reaction mixture was warmed at reflux (100°C) for 1 hour, during which it became a clear solution. MS monitoring revealed no complete conversion; in addition, the pH dropped to pH 4.2. A second portion of 1 M aqueous solution of NaOH (20 μL, 20 μmol, ca 0.3 equiv) was added to adjust to pH 4.7, and the mixture was warmed at reflux (100°C) for an additional 30 min. After cooling to room temperature, the pH again was lowered slightly to 4.5, while the MS and HPLC controls showed incomplete conversion (90%). The aqueous mixture was filtered through a 0.22 μm PES membrane (syringe filter unit) and then lyophilized. The crude material (pale pink solid) was purified on preparative RP-TLC glass plate (H<sub>2</sub>O/MeCN 7/3 v/v). The title compound was recovered from a silica strip corresponding to R<sub>f</sub> 0.20-0.27 ranges (11 mg); HPLC control gave 80% purity with the presence of starting chelating agent (20%). A larger amount of unreacted starting chelating agent was recovered from a silica strip corresponding to R<sub>f</sub> 0.27-0.32 ranges (4 mg, 8.2 μmol). Conversion: 80%; corrected yield: 37%. <sup>1</sup>H NMR (DMSO-d<sub>6</sub>, c ≈ 40 mM, Figure S6): δ(ppm) 9.77 (<1H, br s, (CS)NH-Ar), 8.07 (<1H, br s, (CS)NH-CH<sub>2</sub>), 7.50 (2H, part A of AB system, <sup>3</sup>J = 8.4 Hz, CH<sub>ar</sub>), 7.34 (2H, part A of AB system, <sup>3</sup>J = 8.4 Hz, CH<sub>ar</sub>), 4.48 (1H, part A of AX system, <sup>3</sup>J = 14.5 Hz, CHH), 3.77-3.58 (2H, m, CH<sub>2</sub>), 3.55-3.04 (>9H, several m, N-CH<sub>2</sub> (9H) and H<sub>2</sub>O in DMSO), 2.97-2.64 (7H, m, N-CH<sub>2</sub>), 2.30-2.18 (1H, m, CHH), 1.58-1.46 (2H, m, CH<sub>2</sub>(CH<sub>2</sub>NH)), 1.37-1.26 (2H, m, CH<sub>2</sub>(CH<sub>3</sub>)), 0.90 (3H,

t, <sup>3</sup>J = 7.3 Hz, CH<sub>3</sub>). <sup>13</sup>C{<sup>1</sup>H} NMR (DMSO-d<sub>6</sub>, c ≈ 40 mM, Figure S6): δ(ppm) 179.6, 171.5 (CO, CS), 139.8 (Cquat<sub>ar</sub>), 132.2 (CH<sub>ar</sub>), 128.1 (Cquat<sub>ar</sub>), 121.9 (CH<sub>ar</sub>), 63.8, 63.7, 60.3, 54.1, 52.4, 52.3, 52.1, 51.7, 45.6, 43.4 (CH<sub>2</sub>), 30.5 (CH<sub>2</sub>(CH<sub>2</sub>NH)), 19.6 (CH<sub>2</sub>(CH<sub>3</sub>)), 13.7 (CH<sub>3</sub>). LRMS (MeOH, 40 V): *m/z* 530 [Al-OH-L + Na]<sup>+</sup>, 1037 [2(Al-OH-L) + Na]<sup>+</sup>. HRMS: calculated for [C<sub>22</sub>H<sub>34</sub>AlN<sub>5</sub>O<sub>5</sub>S + H]<sup>+</sup>, *m/z*: 508.21743, found, *m/z*: 508.21510 with *z* = 1; error: 1.78 ppm. HPLC (Figure S8): R<sub>t</sub> 5.5-5.7 min.

**AI-OAc-NODA-MP-C4.** Two stock solutions were prepared in advance, both of them diluted in 0.1 M AcONa/H buffer solution at pH 4.5: i) a 0.0134 M solution of chelating agent NODA-MP-C4 isolated at pH 4.3; ii) a 0.2 M solution of AlCl<sub>3</sub> (resulting pH 2.9). The reaction was performed by mixing the chelating agent (965 μL of the stock solution, ca 13 μmol), AlCl<sub>3</sub> (80 μL of the stock solution, 16 μmol, ca 1.2 equiv). The mixture was diluted by addition of a 0.1 M AcONa/H buffer solution at pH 4.5 (197 μL) and ethanol (138 μL corresponding to 10% v/v of the total reaction volume), then warmed at reflux (100°C) for 30 min followed by room temperature overnight. The crude mixture was lyophilized, then analyzed by LC-MS that confirms the total conversion and the formation of a mixture of Al-OH-NODA-MP-C4 (70%) together with the title compound Al-OAc-NODA-MP-C4 (30%). LRMS (MeOH, 40 V): *m/z* 572 [Al-OAc-L + Na]<sup>+</sup>, 1121 [2(Al-OAc-L) + Na]<sup>+</sup>. HRMS: calculated for [C<sub>24</sub>H<sub>36</sub>AlN<sub>5</sub>O<sub>6</sub>S + Na]<sup>+</sup>, *m/z*: 572.20994, found, *m/z*: 572.20734 with *z* = 1; error: 2.05 ppm. HPLC: R<sub>t</sub> 10.3-10.5 min.

**AI-F-NODA-MP(O)-C4 and AI-OAc-NODA-MP(O)-C4.** Two stock solutions were prepared in advance, both of them diluted in a 0.5 M AcONa/H buffer solution at pH 4.45: i) a 0.100 M solution of AlCl<sub>3</sub> (resulting pH 3.6); ii) a 0.100 M solution of NaF (resulting pH 4.45). The previously isolated chelating agent NODA-MP(O)-C4 (18.0 mg, ca 37 μmol) was solubilized in 0.5 M AcONa/H buffer solution at pH 4.45 (1.63 mL). AlCl<sub>3</sub> (0.100 M previously prepared stock solution, 1.1 mL, 110 μmol, 3 equiv) followed by NaF (0.100 M previously prepared stock solution, 550 μL, 55 μmol, 1.5 equiv) were added. Ethanol was then added in order to represent 10% v/v of the total reaction volume (370 μL). The resulting reaction mixture (pH 4.4) was warmed at reflux (100°C) for 20 min, then cooled, and freeze-dried. The crude material was purified on preparative RP-TLC glass plate (H<sub>2</sub>O/MeCN 7/3 v/v); the title compounds were recovered as a mixture from silica band corresponding to R<sub>f</sub> 0.32-0.46 ranges (10 mg, 50%). LRMS (MeOH, 40 V): *m/z* 516 [Al-F-L + Na]<sup>+</sup>, 556 [Al-OAc-L + Na]<sup>+</sup>, 1009 [2(Al-F-L) + Na]<sup>+</sup>.

**AI-F-NODA-MP(O)-C4.** <sup>19</sup>F{<sup>1</sup>H} NMR (D<sub>2</sub>O, pH 7, Figure S7): δ -165.9. <sup>19</sup>F{<sup>1</sup>H} NMR (DMSO-d<sub>6</sub>, Figure S7): δ -169.7. (LC-)HRMS: calculated for [C<sub>22</sub>H<sub>33</sub>AlFN<sub>5</sub>O<sub>5</sub> + H]<sup>+</sup>, *m/z*: 494.23596, found, *m/z*: 494.2362 with *z* = 1; error: 0.49 ppm. HPLC (Figure S8): R<sub>t</sub> 4.7 min.

**AI-OAc-NODA-MP(O)-C4.** (LC-)HRMS: calculated for [C<sub>22</sub>H<sub>33</sub>AlN<sub>5</sub>O<sub>5</sub>]<sup>+</sup>, *m/z*: 474.22973, found, *m/z*: 474.2300 with *z* = 1; error: 0.56 ppm. HPLC (Figure S8): R<sub>t</sub> 5.6 min.

**AI-OH-NODA-MP(O)-C4.** Similar protocol to that used to prepare the thiourea analog AI-OH-NODA-MP-C4 was applied starting from a 70/30 mol/mol mixture of chelating agents NODA-MP-C4 and NODA-MP(O)-C4 (Na forms) isolated previously at pH 5 (40 mg, ca 82 μmol). Purification by preparative RP-TLC glass plate (H<sub>2</sub>O/MeCN 7/3 v/v) led to the title compound recovered from a silica strip corresponding to R<sub>f</sub> 0.20-0.27 ranges (20 mg). HPLC control gave a ratio of 70/30 for the corresponding thiourea and urea complexes in accordance with the ratio of starting materials involved. Moreover, as previously, conversion was not completed and HPLC control gave 90% purity for chelates with the presence of starting chelating agents (10%). The chromatogram is presented in Figure S8. As previously, a larger amount of unreacted starting chelating agents was recovered from a silica strip corresponding to R<sub>f</sub> 0.27-0.32 ranges (8 mg, 16 μmol). Conversion: 75%; corrected yield: 65%. LRMS (MeOH, 40 V): *m/z* 514 [Al-OH-L + Na]<sup>+</sup>. HRMS: calculated for [C<sub>22</sub>H<sub>34</sub>AlN<sub>5</sub>O<sub>6</sub> + H]<sup>+</sup>, *m/z*: 492.240274, found, *m/z*: 492.23762 with *z* = 1; error: 5.39 ppm. HPLC (Figure S8): R<sub>t</sub> 3.2 min.

## RESEARCH ARTICLE

## Radiolabeling Procedure

[<sup>18</sup>F]F<sup>-</sup> was produced via the [<sup>18</sup>O(p,n)<sup>18</sup>F] nuclear reaction for 10-15 min with a cyclotron (Cyclone 18/9, IBA). 10-30 GBq in a 2.2 mL volume arrived in the automated synthesizer (AllinOne, Trasis) for purification and elution of the [<sup>18</sup>F]NaF. [<sup>18</sup>F]F<sup>-</sup> was loaded onto a QMA cartridge (Sep-Pak Accell Plus QMA Plus Light, Waters) equilibrated with ultrapure water. After the loading, sample was rinsing with 5 mL ultrapure water to remove any dissolved impurities. [<sup>18</sup>F]F<sup>-</sup> was then eluted with 2 mL of saline 0.9% in a vial that has been placed in a shield container beforehand. Radioactivity of the final product was measured with a dose calibrator (PET Dose 5 Ci, COMECER). Several 2mM AlCl<sub>3</sub> and NODA-MP-C4 stock solutions were prepared by dissolving respectively AlCl<sub>3</sub>·6H<sub>2</sub>O and NODA-MP-C4 in 0.1M AcONa/H solution with different pH (4.0; 4.2; 4.3; 4.5; 4.8; 5.0). Working solution were prepared based on the table generated by the DoE software (Ellistat®). Radiolabeling was performed by adding AlCl<sub>3</sub> (stock solution, 30 μL) of NODA-MP-C4 (stock solution, 30 μL) and [<sup>18</sup>F]NaF (50 μL, about 500 MBq) to the reactor. Then, reaction mixture was placed in an open reactor (glass test tube type so that the fixed temperature was rapidly attained in less than 2 minutes) and warmed at reflux (100°C) for 15 min. After reaction cooling with compressed air, RCC was determined using radio-HPLC. The identity of Al<sup>18</sup>F-NODA-MP-C4 was confirmed by co-injection with its cold reference synthesized, Al<sup>19</sup>F-NODA-MP-C4. RCC was determined based on the relative percentage area of the compound peak. Chromeleon™ data system software (version 6.8) was used for data acquisition and mathematical calculations.

## DoE Design

DoE study was designed and analyzed using Ellistat® version 6.8 to maximize the RCC. Three experimental factors were investigated: pH (pH, 4 – 5), the concentration of the chelating agent derived from NODA ([NODA-MP-C4], 50 – 550 μM) and chelating agent/aluminum ratio (NODA-MP-C4 / AlCl<sub>3</sub>, 1 / 1 – 3 / 1). The central composite design was chosen due to its ability to estimate with high precision quadratic terms in the response surface design though it requires a higher number of tests than other designs. This design consisted of a total of 20 tests: 8 factorial points, 6 center points and 6 axial points. We decided to duplicate the tests to improve the predictive model. Experiments were performed in randomized order over 5 days. The response was the RCC that was determined by radio-HPLC method as described below. The model was fitted using multiple linear regression. The model was based on the full multiple polynomial regression, which includes all the quadratic terms and interactions terms. Depending on the t-statistic which reflects the significant impact of the term on the response, each term is kept or removed from the equation to achieve a simple and fitting model.

## Supporting Information

The authors have cited additional references within the Supporting Information.<sup>[6,17,22,23]</sup>

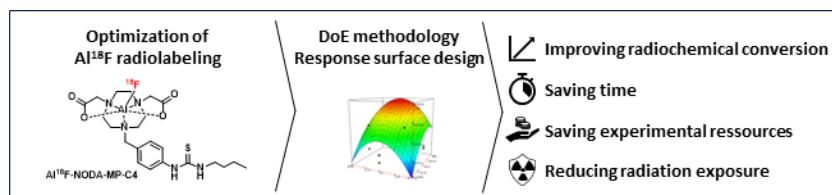
## Acknowledgements

We thank Anne Regazzetti and Violette Haldys (U-Paris Cité, Faculté des Sciences Pharmaceutiques et Biologiques mass-spectroscopy platform) for (LC-)HRMS analyses. The research was supported by Comité de Paris de la Ligue contre le Cancer and by ITMO Cancer of Aviesan on funds administered by Inserm.

**Keywords:** NODA • aluminum • fluorine-18 • radiochemistry • design of experiments

- [1] A. Sanchez-Crespo, *Appl. Radiat. Isot.* **2013**, *76*, 55–62.
- [2] K. R. Scroggie, M. V. Perkins, J. M. Chalker, *Front. Chem.* **2021**, *9*, 687678.
- [3] A. C. A. Bispo, F. A. F. Almeida, J. B. Silva, M. Mamede, *Int. J. Org. Chem.* **2022**, *12*, 161–172.
- [4] W. J. McBride, R. M. Sharkey, H. Karacay, C. A. D'Souza, E. A. Rossi, P. Laverman, C.-H. Chang, O. C. Boerman, D. M. Goldenberg, *J. Nucl. Med.* **2009**, *50*, 991–998.
- [5] C. Fersing, A. Bouhlel, C. Cantelli, P. Garrigue, V. Lisowski, B. Guillet, *Molecules* **2019**, *24*, 2866.
- [6] D. Shetty, S. Y. Choi, J. M. Jeong, J. Y. Lee, L. Hoigebazar, Y.-S. Lee, D. S. Lee, J.-K. Chung, M. C. Lee, Y. K. Chung, *Chem. Commun.* **2011**, *47*, 9732–9734.
- [7] W. J. McBride, C. A. D'Souza, R. M. Sharkey, H. Karacay, E. A. Rossi, C.-H. Chang, D. M. Goldenberg, *Bioconjugate Chem.* **2010**, *21*, 1331–1340.
- [8] P. T. Huynh, N. Soni, R. Pal, S. Sarkar, J.-M. Jung, W. Lee, J. Yoo, *New J. Chem.* **2019**, *43*, 15389–15395.
- [9] Z. Zha, S. R. Choi, K. Ploessl, D. Alexoff, R. Zhao, L. Zhu, H. F. Kung, *Bioconjugate Chem.* **2021**, *32*, 1017–1026.
- [10] D. Kang, U. Simon, F. M. Mottaghy, A. T. J. Vogg, *Pharmaceuticals* **2021**, *14*, 818.
- [11] G. D. Bowden, B. J. Pichler, A. Maurer, *Sci. Rep.* **2019**, *9*, 11370.
- [12] C. J. Taylor, A. Pomberger, K. C. Felton, R. Grainger, M. Barecka, T. W. Chamberlain, R. A. Bourne, C. N. Johnson, A. A. Lapkin, *Chem. Rev.* **2023**, *123*, 3089–3126.
- [13] M. M. Herth, S. Ametamey, D. Antuganov, A. Bauman, M. Berndt, A. F. Brooks, G. Bormans, Y. S. Choe, N. Gillings, U. O. Häfeli, M. L. James, K. Kopka, V. Kramer, R. Krasikova, J. Madsen, L. Mu, B. Neumaier, M. Piel, F. Rösch, T. Ross, R. Schibli, P. J. H. Scott, V. Shalgunov, N. Vasdev, W. Wadsak, B. M. Zeglis, *Nucl. Med. Biol.* **2021**, *93*, 19–21.
- [14] F. Chen, Y. Xiao, K. Shao, B. Zhu, M. Jiang, *J. Labelled Compd. Radiopharm.* **2020**, *63*, 494–501.
- [15] W. Wang, Z. Liu, Z. Li, *Bioconjugate Chem.* **2015**, *26*, 24–28.
- [16] W. Wan, N. Guo, D. Pan, C. Yu, Y. Weng, S. Luo, H. Ding, Y. Xu, L. Wang, L. Lang, Q. Xie, M. Yang, X. Chen, *J. Nucl. Med.* **2013**, *54*, 691–698.
- [17] D. Shetty, J. M. Jeong, Y. J. Kim, J. Y. Lee, L. Hoigebazar, Y.-S. Lee, D. S. Lee, J.-K. Chung, *Bioorg. Med. Chem.* **2012**, *20*, 5941–5947.
- [18] J. Guo, L. Lang, S. Hu, N. Guo, L. Zhu, Z. Sun, Y. Ma, D. O. Kiesewetter, G. Niu, Q. Xie, X. Chen, *Mol. Imaging Biol.* **2014**, *16*, 274–283.
- [19] L. Lang, Y. Ma, D. O. Kiesewetter, X. Chen, *Mol. Pharmaceutics* **2014**, *11*, 3867–3874.
- [20] S. Schmitt, E. Moreau, *Coord. Chem. Rev.* **2023**, *480*, 215028.
- [21] E. Callegari, J. Martinelli, N. Guidolin, M. Boccalon, Z. Baranyai, L. Tei, *Molecules* **2023**, *28*, DOI 10.3390/molecules28093764.
- [22] A. Bodor, I. Tóth, I. Bányai, Z. Szabó, G. T. Hefter, *Inorg. Chem.* **2000**, *39*, 2530–2537.
- [23] U. Kreher, M. T. W. Hearn, B. Moubaraki, K. S. Murray, L. Spiccia, *Polyhedron* **2007**, *26*, 3205–3216.

## Entry for the Table of Contents



**Lesser, better, faster:** Optimization of a radiolabeling method by complexation of aluminum- $[^{18}F]$ fluoride  $\{Al^{18}F\}$  species using a Design of Experiments (DoE) approach. This study demonstrates the potential of this strategy in radiochemistry for optimization of a radiochemical process.

Institute and/or researcher Twitter usernames: @LeCnam